IOP Publishing European Journal of Physics
Eur. J. Phys. **45** (2024) 045703 (11pp) https://doi.org/10.1088/1361-6404/ad4931

The potential of a uniformly charged planar structure with shape of a rose curve

Sheng Chen[1], **Yanyi Wu**[1], **Xin Chang**[2] and **Baohua Teng**[1,2]

[1] School of Physics, University of Electronic Science and Technology of China, Chengdu 611731, People's Republic of China
[2] Yingcai Experimental School, University of Electronic Science and Technology of China, Chengdu 611731, People's Republic of China

E-mail: chensheng9807@163.com

Received 25 June 2023, revised 7 April 2024
Accepted for publication 9 May 2024
Published 28 May 2024

Abstract

The electric potential $U(\theta)$ of a uniformly charged plane with a rose-curve shape (referred to as a 'rose disk') satisfies a 'roselike curve function,' and there exists an asymptotic expression for the potential when the observation point is far from the rose disk. To validate the accuracy of the model, a constant electric current field was employed to simulate the electrostatic field. The potential distribution characteristics of uniformly charged circular discs and trilobal rose discs in the experimental setting were equivalently obtained by the experiment of electrolytic tank. The results indicate that under the non-idealized constraints of real experimental conditions, the asymptotic formula can be used as an analytical method to quickly study the rose disk potential.

Keywords: rose disk, potential curve, electrostatic field simulation

1. Introduction

In the field of electrostatics, the study of the potential distribution of uniformly charged bodies is a classical topic, and it holds significant importance for the development and improvement of electronic engineering devices. For uniformly charged polygonal planes [1], such as triangles [2] and rectangles [3], the potential analytical expression can be obtained by using either the direct integration method or the superposition principle. However, for structures with a rose-curve shape and many blades, the potential may not be obtained by analytical methods. Therefore, for charged bodies with intricate boundary conditions and geometric

shapes, it is common to employ Maxwell's and Laplace's equations and utilize the relaxation method for numerical solutions [4–6].

While the relaxation method iteratively solves the precise differential equations to obtain numerical values of the electromagnetic field, it demands substantial computational resources and time, and lacks sufficient interest in educational contexts. Moreover, from a physical perspective, solving the electromagnetic potential of a complex charged body may not have significant value. This is because such results often lack specific mathematical functional forms, providing only quantitative calculations. Therefore, in physics education and the field of electronic engineering where high precision is not crucial, obtaining approximate analytical formulas for the electromagnetic potential of complex structures is essential [3], even though these results may only be applicable in specific cases.

In practice, users desire to simultaneously measure and identify the structure of objects. With the asymptotic analytical formulation of this problem, we can rapidly achieve numerical estimation of the electromagnetic field, which can be utilized to derive model inversely from the potential field. This data inversion approach holds broad prospects for applications, especially in the fields of magnetotellurics and metal detection. It is possible to characterize metallic objects embedded in an infinitely homogeneous conducting ground and to measure the scattering information [7–9] or electromagnetic potential information at low frequencies of metallic bodies in a conducting medium by using electromagnetic induction. Deciphering these fields facilitates the localization and estimation of parameters such as size, orientation, shape, and conductivity of the embedded structure.

In addition to purely mathematical methods such as approximation methods, methods for quickly solving field distributions of specific complex shaped electrodes include simulation methods, such as the experiment of electrolytic tank [6, 10–16]. In principle, this method is based on the analogy between the constant current field and other potential fields, such as electrostatics, magnetostatics, temperature, fluid dynamics, and gravity. It can be employed to determine the solution of Laplace equation with specific boundaries in a homogeneous medium [17]. The advantage of this experimental setup lies in the simplicity of changing electrode configurations with different geometric shapes. It can quickly and accurately solve the problems that cannot be analyzed by pure analytical methods. In addition to education in electrostatics, this method also provides experience in industrial equipment manufacturing at a low experimental cost. For instance, in electrical engineering, this method can also be used for the determination of electric stress and pulse voltage in power transformers, based on analogies between the resistance, current, inductance and magnetoresistance, electric flux, capacitance in the electrolyte [13]. The distribution of fringing fields is altered by adjusting the shape of complex components. It provides necessary insulation for transformer winding equipment [16]. Additionally, in mechanical engineering, electrolytic tanks offer an alternative solution. By using equipotential lines to represent the incompressible flow lines of the fluid, the impact of blade shape and inlet/outlet angles on performance can be assessed through the analysis of pressure and velocity distributions under these conditions. This eliminates the need for wind tunnel experiments to obtain the required design information [15, 16].

The use of an electrolytic tank experiment in the classroom is not only to validate the effectiveness of the asymptotic formula for electromagnetic potential discussed in this paper but more importantly, to combine theoretical and experimental simulation. This approach can greatly stimulate the interest of teachers and students, and cultivate the students' ability in scientific research and practice. Simultaneously, providing clearer field diagrams for students to facilitate a more effective exploration of the electromagnetic phenomena of charged objects. This helps them to understand the basic principles and concepts of electrostatics more

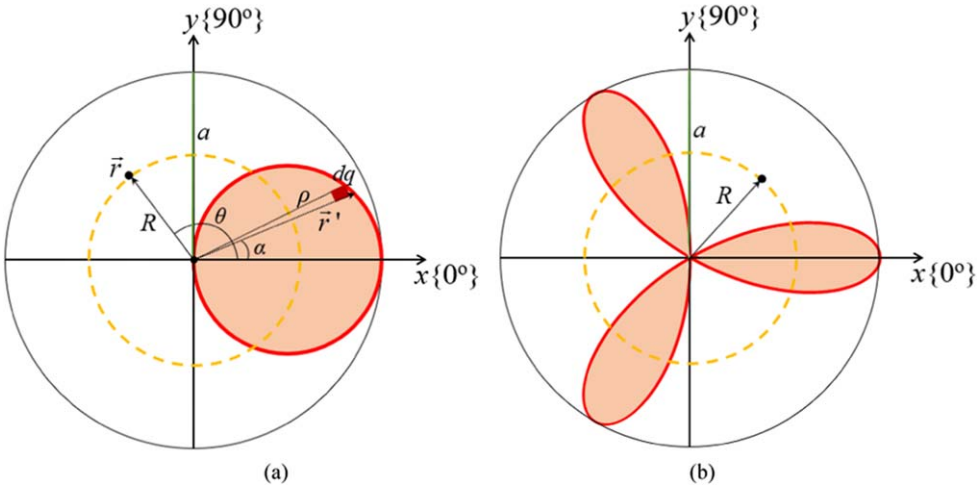

Figure 1. Illustration diagram of position of the field point, where the red curve represents the contour of the charged body, and the field point is located on a circle of radius R (yellow curve). (a)circular disk: $\rho = a\cos(\alpha)$; (b) three-petal rose disk: $\rho = a\cos(3\alpha)$.

deeply [12, 18]. Based on this experimental method, previous studies have predominantly focused on investigating the distribution of the same potential within a plane on electrodes of certain shapes. This involves the relationship between equipotential lines and the shape of the charged body, thereby confirming the interdependence of field sources [1, 11, 12]. However, due to the constraints of the electrode shapes in this classic experiment [11, 19] and the entrenched mindset of traditional teaching, they did not delve deeply into the distribution of potentials on the defined paths in the electrolytic tank, i.e. the relationship between the potential curves and the shapes of charged objects.

2. Models and formulas

The analytical approach presented in this paper is applicable for dealing with uniformly charged planar structures with a contour in the shape of a rose curve $\rho = a\cos(n\alpha)$ (a is the envelope radius of the rose disk, and n is an integer indicating the number of leaves). By straightforward transformations, the corresponding results of this geometric figure can be easily extended to some special cases [7]. Simultaneously, for the application of this paper, we aim for measurement results to be sensitive only to general information of the structure, such as overall shape and average conductivity. As one of the typical standard shapes, the results of the rose disk can reproduce well the orientation, size, shape, conductivity and other characteristics of the original figure.

In figures 1(a) and (b), we respectively depict uniformly charged planes with rose curve contours for $n = 1$ and $n = 3$ in polar coordinates. We investigate the potential distribution on a circle of radius R centered at the pole (for $n = 1$, the pole is the edge point of the disk, and for $n = 3$, the pole is the center of the rose disk).

The integral of the electric potential is defined by $V = \int \mathrm{d}q/4\pi\varepsilon_0|\boldsymbol{r} - \boldsymbol{r'}|$. The point charge microelements on the rose disk are $\mathrm{d}q = \sigma \mathrm{d}S = \sigma\rho \mathrm{d}\rho d\theta$, and the position vector is $\boldsymbol{r'}(\rho\cos\alpha, \rho\sin\alpha)$. Then integrate over the closed region enclosed by the rose curve. Thus, for the point

with radius-vector $\boldsymbol{r}(R\cos\theta, R\sin\theta)$ on a concentric circle with the center at the heart of the rose disk and a radius of R, the electric potential can be expressed as:

$$U(R,\theta)=\frac{\sigma}{4\pi\varepsilon_0}\int_0^{2\pi}\int_0^{a\cos(n\alpha)}\frac{\rho}{\sqrt{(\rho\cos\alpha-R\cos\theta)^2+(\rho\sin\alpha-R\sin\theta)^2}}\mathrm{d}\rho\mathrm{d}\alpha, \tag{1}$$

where σ denotes the charge surface density of the rose disk and ε_0 is the permittivity in vacuum. If the radius R of the concentric circle is constant, the electric potential is a unary function about the polar angle θ, which is recorded as $U(\theta)$. For this double parametric integral, which is difficult to solve analytically, the potential distribution can be determined through numerical calculations. Extensive numerical validations have been performed using Python programs in the appendix, and concluded that there exists an asymptotic formula for equation (1) at $R \gg a$:

$$U(\theta)\simeq\begin{cases}A\cos(n\theta)+B, & n\ \text{is odd}\\ A\cos(2n\theta)+B, & n\ \text{is even}\end{cases} \tag{2}$$

where $A=(U_{\max}-U_{\min})/2$ and $B=(U_{\max}+U_{\min})/2$, $U_{\max}$ and $U_{\min}$ correspond to the maximum and minimum values of the electric potential at a given field point on the circles, respectively. It is not difficult to conclude that when n is odd, the electric potential reaches its maximum value $U_{\max}$ at $\theta_O=2k\pi/n$ and its minimum value $U_{\min}$ at $\theta_O=(\pi+2k\pi)/n$. When n is even, the electric potential reaches its maximum value $U_{\max}$ at $\theta_E=k\pi/n$ and its minimum value $U_{\min}$ at $\theta_E=(\pi+2k\pi)/2n$.

From calculations of equations (1) and (2), it can be observed that, for a charged plane with a blade shape, both the equipotential lines near the source and the potential lines far away from the source exhibit characteristics similar to the contours of the charged plane. This similarity can be utilized to analyze the charged characteristics of the object and the distribution of the electric field. Simultaneously, these two aspects can complement each other in spatial extent. In engineering, the appropriate electrode shape can be selected according to this law which aims to produce the desired target field in specific regions. However, it is worth noting that, from an experimental perspective, potential curves offer more useful information compared to equipotential lines. Potential curves possess specific mathematical functions, making the comparison between experimental and theoretical values more convenient.

3. Experimental simulation

The experimental setup [16] for simulating electrostatic potential using the sink method is illustrated in figure 2. To balance cost-effectiveness and teachability, we opted for two shapes of electrodes, a circle disk made of thin iron sheets and a trilobal rose disk. The radius of the circle is 1.3 cm, and the enveloping radius of the trilobal rose is 2.0 cm, with tap water serving as the electrolyte. In the experiment, the electrodes are immersed into the water tank, which is covered with graph paper at the bottom. They are positioned as centrally as possible within the basin. The positive pole of the constant voltage source is directly connected to the iron sheets, ensuring that the iron sheets share the same electric potential. Therefore, the experimental setup is suitable for measuring situations where $R/a \geqslant 1$. The metal ring embedded in the water tank wall serves as the negative electrode of the closed circuit. Its electric potential is set to zero (or grounded) to meet the Dirichlet boundary condition [6].

As the conductivity of water is significantly lower than that of iron, it can be assumed that the electric field strength inside the electrodes can be considered to be zero. A uniform field is

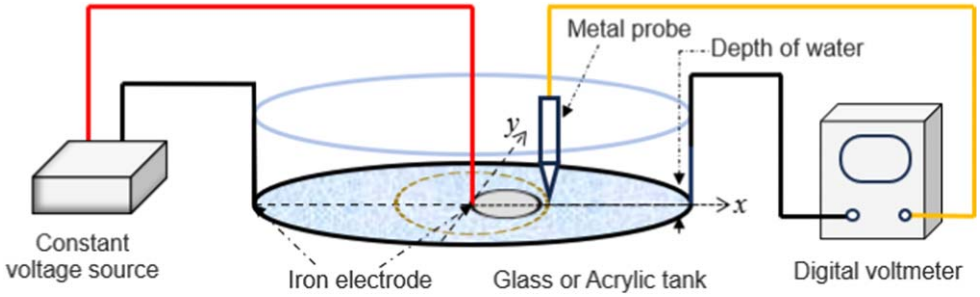

Figure 2. Diagram of the experimental setup for the electrolytic tank experiment (the conductors are represented by lines of different colors).

formed within the electrolyte, and the electric potential satisfies the Laplace equation. The distribution of electrostatic potential is equivalent to the distribution of current, and its qualitative characterization can be determined using a voltmeter. During the experiment, one end of the voltmeter is connected to the negative electrode of the water tank wall, and the other end of the voltmeter is connected to the probe. By measuring the potential values at specified locations in the electrolyte, the variation in electric potential along a specific path can be determined. Specifically, in this experiment, we measured the electric potential generated by electrodes in the shapes of a circular disk and a trilobal rose disk on a circle at a distance r from the center of the water tank.

The division value of the digital voltmeter is 0.01 V, in order to reduce the relative error, the constant voltage set in this experiment should not be too small, and it should not be too large in order to avoid the potential risks caused by the students' misoperations at the same time. The voltage between the two electrodes in the water tank of the experiment is maintained at around 10 V. Additionally, low-frequency alternating current voltage reduces the ionization of water and polarization effects of the electrode surfaces [14]. Although tap water may not be considered as a uniformly conductive medium similar to that in electrostatic theory, this factor is negligible compared to other errors for physics teaching experiments [20]. Compared to conductive and silicon gels, liquid electrolytes require that the experimental bench be placed on a sufficiently level surface. Additionally, it is preferable for the liquid to submerge the electrodes completely to ensure symmetry and form a two-dimensional field. When the water surpasses the height of the electrodes, the region directly above the electrodes no longer acts as an equipotential surface. The water is so deep that the measured potential is directly above the point, and the potential law does not satisfy equation (1). Moreover, the tip of the probe should be extremely fine. This operation not only reduces the error of taking points, but also eliminate the meniscus caused by surface tension when the probe contacts the liquid. This helps avoid uneven electric fields caused by the non-uniformity of the electrolyte. Additionally, the fine tip also helps to minimize field disturbances and potential measurement errors caused by probe insertion [13].

4. Results and error analysis

Based on the point selection strategy shown in figure 1 and the measurement plan outlined in figure 2, we first chose points ($a = 1.3$ cm, $R = 5.0$ cm) on a circle with a radius of 5.0 cm centered on the edge of the circular electrode as the field points for measuring potential. Subsequently, for the trilobal rose disk electrode, the potential ($a = 2.0$ cm, $R = 2.0$ cm) was

Table 1. Potential measurement values for the circular and trilobal rose discs (circular disc: $a = 1.3$ cm, $R = 5.0$ cm, trilobal rose disc: $a = 2.0$ cm, $R = 2.0$ cm).

	Angle°								
Electric potential V	0	20	40	60	80	100	120	140	160
Disk	6.98	6.89	6.78	6.55	6.35	6.00	5.75	5.53	5.25
Three-leaf rose plate	7.41	7.31	7.12	6.95	7.18	7.27	7.35	7.29	7.16
	Angle°								
Electric potential V	180	200	220	240	260	280	300	320	340
Disk	5.13	5.09	5.28	5.56	5.98	6.21	6.48	6.77	6.86
Three-leaf rose plate	6.99	7.04	7.18	7.41	7.22	7.04	6.96	6.99	7.26

measured on a concentric circle to this electrode and with a radius equal to the enveloping radius. Starting along the polar axis, potential measurements were taken at every 20° points, and the measured data were shown in table 1.

In order to compare the results of the integral, asymptotic and experimental values, we need to perform a uniform normalizing transformation of the potential values: $U' = (U - U_{\min})/(U_{\max} - U_{\min})$. Subsequently, in the polar coordinate system of figure 3, the measured experimental values, the integral values obtained using the defining equation (1) of potential, and the asymptotic values calculated using equation (2) were simultaneously plotted as a function of angle.

From figure 3, it can be observed that both the directly integrated values and the asymptotic values qualitatively match the characteristic of potential distribution of the uniformly charged rose disk obtained in the experiment. Specifically, the potential curve for the circular disk exhibits a heart-shaped line, while the potential curve for the rose disk exhibits a rose-shaped line. However, in terms of numerical values, there is a significant error between the experimental values and the directly integrated values, while there is a higher degree of agreement with the asymptotic values. This is because there exists a significant disparity between experimental conditions and theoretical assumptions in practical educational experiments. Therefore, there will be some deviation between actual results and ideal theoretical solutions. We believe that the experimental results should be compared with the solutions obtained by considering the experimental conditions, rather than with the ideal theoretical solution [6, 12].

Electrodes handmade by students were employed. Due to the imperfect match between the shape of these electrodes and standard components, it may lead to slight deformation and displacement of the potential curves. However, due to its unique shape and symmetry, its outcomes do not mislead us in analyzing the actual electric field distribution of the charged rose-shaped body. Quantitatively, the crucial matter we are concerned with is that: (i) when R/a is not too large, the potential curve satisfies the case of $R \gg a$ better. In other words, equation (2) converges more quickly under experimental conditions. (ii) A larger number of leaves also causes equation (2) to reach convergence more quickly as R/a increases. However, why is there less agreement between the experimental values and asymptotic values for the three-petal rose disk compared to the circular disc? Therefore, an equivalent circuit diagram of this experimental setup is plotted in figure 4, which analyzes and explains the effect of this experimental condition on the results.

The tendency of experimental values to approach asymptotic values can be attributed to the following reasons. On the one hand, the voltmeter used in the experiment is not an ideal one, but there is an internal resistance R_V. The voltmeter shares a portion of the current in the

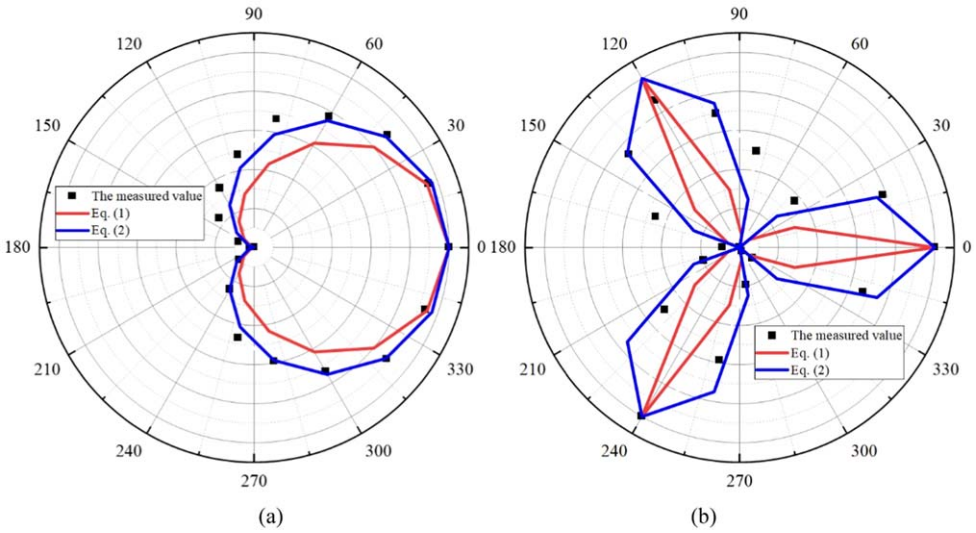

Figure 3. Potential curves $U'(\theta) \sim \theta$ of the rose disk obtained from experimental measurements and theoretical calculations.

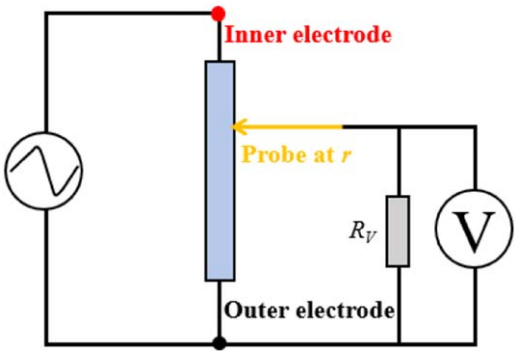

Figure 4. The equivalent circuit diagram of electrolytic tank which corresponds to figure 2.

electrolyte, which leads to the measured potential value being smaller than the theoretical value. Therefore, the asymptotic condition *R/a* required in the potential law equation (2) is smaller than the theoretical value. In the same experimental setup, to minimize the systematic error caused by the internal resistance of the voltmeter, a conductive medium with higher resistivity, such as gel [11], was employed. Alternatively, for the same isotropic medium, a larger water tank (theoretically, the negative pole should be connected to infinity) was selected. This will increase the resistance from the electrode to the wall of the tank due to the increased distance. During the movement of the probe from the center electrode to the edge, the combined resistance of the voltmeter's internal resistance and the electrolyte resistance approximates the resistance of the electrolyte. At this point, the current passing through R_V decreases, and the potential value displayed by the voltmeter becomes closer to the potential at position r in ideal conditions.

On the other hand, the existence of differences is also related to the limited size of the water tank, meaning that the boundary conditions are not idealized [6]. Equivalence between electrostatic and current fields only holds automatically in infinite space. Obviously, from an educational perspective, the conductivity of the water and electrodes, as well as the shape and size of the electrodes and electrolytic tank are taken into account, deriving the exact solution is a laborious and futile task, so we have abandoned the precise fitting of the potential solution. The three-leaf rose disk used in the experiment is larger in size, and the distance between the central electrode and the wall of tank is closer. The electric field in the water rapidly attenuates, and the electrolyte exhibits a greater potential gradient along the radial direction. As a result, the potential law, which would typically need to be satisfied on concentric circles of larger radius, is satisfied in this experiment only as long as the field points are not too close to the electrode. This situation, however, leads to the asymptotic results also falling short of the ideal outcome. To better reproduce the ideal state, smaller electrode model dimensions were adopted [20]. In this scenario, the boundary of electrolytic tank is equivalent to an infinite boundary for it, and the disturbance caused by the electrode being far from the boundary approximates isolation [10]. This way, the potential at a distance from the electrode simultaneously conforms to both the integral value (1) and the asymptotic value (2).

5. Conclusion

This paper initially employs numerical analysis methods to investigate the electric potential of a uniformly charged rose disk in a two-dimensional space, and the asymptotic analytical expression is obtained under limiting conditions. The expression undergoes only straightforward transformations with the original graphical function. The expression fully reflects the characteristics of the original graph and can be used for data inversion in practical engineering applications. Additionally, the degree of agreement of this model in experimental conditions is investigated through an electrolytic tank experiment. It was observed that under non-idealized boundary conditions, the potential measurements may be closer to asymptotic values rather than directly integrated values. This suggests that the asymptotic formula can be used as an analytical method to quickly study the rose disk potential. Only when the distance between the electrode and the wall of tank is equivalent to infinity for the electrode size, do the electrostatic field and the current field become fully equivalent, and the difference between the asymptotic values, integral values, and the experimental value disappears.

While many students recognize the correlation between potential distribution and the shape of charged bodies, this concept has not broken the traditional mindset which uses the geometric center as the reference point. As a result, there is not enough understanding of the law of potentials. By analyzing the potential with the edge of the disk as the reference point in a polar coordinate system, specific and aesthetically valuable results were obtained. On the basis, this paper qualitatively and quantitatively analyzes the experimental results of simulating the electrostatic field using the current field, revealing a more general connection between the distribution of electric potential and electric field and the shape of charged bodies. As a result, although this study may have certain limitations, we hope to provide valuable inspiration for students and provide useful references for practical applications of electrolytic tank experiments.

Acknowledgments

The authors would like to thank the Physics Experimental Center of the University of Electronic Science and Technology of China for providing the experimental equipment and Professor Chen Zhongjun of the School of Physics for her valuable insight and discussion on the experimental analysis part.

Data availability statement

All data that support the findings of this study are included within the article (and any supplementary files).

Appendix. Python code

```
from scipy import integrate
  import math
  import matplotlib.pyplot as plt
  (a, n) = (1, 3)
  R = 5
  def db(z):
   def f(x, y):
        return     x/(math.sqrt(((x*math.cos(y)-R*math.cos(z))**2)
+((x*math.sin(y)-R*math.sin(z))**2)))
   def h(y):
   return a*math.cos(n*y)
   v, err = integrate.dblquad(f, 0, 2*math.pi, lambda y: 0, h)
   return v
  def db_y_j(a, b, n_j):
   return a*math.cos(n*n_j)+b
  def db_y_o(a, b, n_o):
   return a*math.cos(2*n*n_o)+b
  db_value_i = []
  db_value_j = []
  db_value_o = []
  tT_i = [i for i in range(0,360)]
  tT_value_i = []
  tT_value_j = []
  tT_value_o = []
  for i in tT_i:
   i_radian = math.radians(i)
   tT_value_i.append(i_radian)
   u_1 = db(i_radian)
   db_value_i.append(u_1)
  U_max = max(db_value_i)
  U_min = min(db_value_i)
  print(U_min, U_max)
  A = (U_max-U_min)/2
  B = (U_max+U_min)/2
```

```
if n % 2 ! = 0:
 for j in tT_i:
 i_radian_j = math.radians(j)
 tT_value_j.append(i_radian_j)
 u_j = db_y_j(A, B, i_radian_j)
 db_value_j.append(u_j)
if n % 2 == 0:
 for o in tT_i:
 i_radian_o = math.radians(o)
 tT_value_o.append(i_radian_o)
 u_o = db_y_o(A, B, i_radian_o)
 db_value_o.append(u_o)
plt.figure(figsize = (6,6))
plt.polar(tT_value_i,db_value_i)
plt.polar(tT_value_j,db_value_j,linestyle = '--')
plt.polar(tT_value_o,db_value_o,linestyle = '--')
plt.ylim(U_min, U_max)
plt.show().
```

ORCID iDs

Sheng Chen https://orcid.org/0009-0006-5425-5940
Yanyi Wu https://orcid.org/0000-0002-6102-3615

References

[1] Sheng C, Junyi L, Xin C, Yanyi W and Baohua T 2023 Spatial potential of arbitrary uniformly charged polygons *Eur. Phys. J. Plus* **138** 1012
[2] Kim U R, Han W, Jung D-W, Lee J and Yu C 2021 Electrostatic potential of a uniformly charged triangle in barycentric coordinates *Eur. J. Phys.* **42** 045205
[3] Fagundes D A 2022 Electrostatic potential of a rectangular uniformly charged plate: exact solution and limiting cases *Eur. J. Phys.* **43** 015203
[4] MacDonald W M 1994 Discretization and truncation errors in a numerical solution of Laplace's equation *Am. J. Phys.* **62** 169–73
[5] DiStasio M and McHarris W C 1979 Electrostatic problems? Relax! *Am. J. Phys.* **47** 440–4
[6] Gil S, Saleta M E and Tobia D 2002 Experimental study of the Neumann and Dirichlet boundary conditions in two-dimensional electrostatic problems *Am. J. Phys.* **70** 1208–13
[7] Vafeas P, Perrusson G and Lesselier D 2009 Low-frequency scattering from perfectly conducting spheroidal bodies in a conductive medium with magnetic dipole excitation *Int. J. Eng. Sci.* **47** 372–90
[8] Perrusson G, Vafeas P and Lesselier D 2010 Low-frequency dipolar excitation of a perfect ellipsoidal conductor *Q. Appl. Math.* **68** 513–36
[9] Vafeas P, Papadopoulos P K and Lesselier D 2012 Electromagnetic low-frequency dipolar excitation of two metal spheres in a conductive medium *J. Appl. Math.* **2012** 1–37
[10] Atwater H A 1968 Laboratory exercises in classical electromagnetic field theory *Am. J. Phys.* **36** 672–82
[11] Elizalde-Torres J, González-Cardel M, Vega-Murguía E J, Castillo-González I and Rodríguez-Nava M 2015 A conductive gel for the plotting of equipotential lines *Phys. Educ.* **50** 468–71
[12] Murata H and Sakuraoka M 1980 Electrostatic potential on a laboratory measurement experiment *Am. J. Phys.* **48** 763–6

[13] Hachemeister C 1955 The application of the electrolytic tank to the solution of potential field problems *Ann. NY Acad. Sci.* **60** 937–47
[14] Sander K F and Yates J G 1953 The accurate mapping of electric fields in an electrolytic tank *Proc. IEEE*II **100** 167–75
[15] Liebmann G 1953 Electrical analogues *Br. J. Appl. Phys.* **4** 193–200
[16] Diggle H and Hartill E R 1954 Some applications of the electrolytic tank to engineering design problems *Proc. IEEE*II **101** 349–64
[17] McDonald D 1953 The electrolytic analogue in the design of high-voltage power transformers *Proc. IEEE*II **100** 145–66
[18] Campos E, Zavala G, Zuza K and Guisasola J 2020 Students' understanding of the concept of the electric field through conversions of multiple representations *Phys. Rev. Phys. Educ. Res.* **16** 010135
[19] Thomas B R 2006 Quantitative electric field measurements in an intermediate laboratory *Am. J. Phys.* **74** 255–9
[20] Einstein P A 1951 Factors limiting the accuracy of the electrolytic plotting tanks *Br. J. Appl. Phys.* **2** 49–55